

## Principles Governing Auditory Cortex Connections

Charles C. Lee and Jeffery A. Winer

Division of Neurobiology, Department of Molecular and Cell Biology, University of California at Berkeley, Berkeley, CA 94720-3200, USA

**Topographic maps are common constituents of the primary auditory, visual, and somatic sensory cortex. However, in most cortical areas, no such maps have yet been identified, posing a conceptual problem for theories of cortical function centered on topography. What principle guides the organization of these other areas? We investigated this issue in cat auditory cortex. The connectional topography of five tonotopic areas and eight non-tonotopic areas was assessed using retrograde tract tracing and quantified by three metrics: clustering, dispersion, and separation. Clustering measures the spatial density of labeled neurons, dispersion provides an index of their spread, and separation serves as a scaling metric. These parameters each show that all auditory cortical regions receive precise and equally topographic connections from thalamic, corticocortical, and commissural sources. This isotropic principle suggests a common substrate for coordinating communication across the cortex and may reflect common mechanisms related to the developmental patterning of connections. This unifying principle extends to auditory and prefrontal cortex, and perhaps to other neocortical areas.**

**Keywords:** maps, thalamus, tonotopy, topography

### Introduction

Topographic representations (maps) are a cardinal feature of mammalian primary auditory (Merzenich *et al.*, 1975), visual (Hubel and Wiesel, 1962), and somatic sensory (Kaas *et al.*, 1979) cortex. Such maps are constructed from neural ensembles with similar physiological properties and that receive topographic anatomical connections from the thalamus and cortex. Each modality contains multiple areas with maps that differ in their topography (Tusa *et al.*, 1978), degree of completeness (Tusa *et al.*, 1979) and functional arrangement (Kaas, 1982). By comparison, topographic physiological maps have not yet been identified in several other auditory, visual, and somatic sensory areas, which thus appear either devoid of maps, have degraded representations or represent some other, as yet undocumented, form of organization (Peters and Jones, 1985). These areas without such well-defined maps are more numerous, and their prevalence suggests that functional mechanisms other than topographic connections may organize them (Kaas, 1997). In areas with emergent or computationally derived maps (Malonek *et al.*, 1994), it is unclear whether their establishment requires topographic connectivity. Thus, if topographic connections are indeed essential for cortical function (Obermeyer and Sejnowski, 2001; Grove and Fukuichi-Shimogori, 2003), then their existence in areas devoid of functional topographic maps remains to be established. Here we present evidence for precise and comparable patterns of connectional topography in 13 areas of the cat auditory cortex

and in the prefrontal and inferior frontal cortex. This topography is present in the thalamocortical, ipsilateral corticocortical, and commissural systems. Its ubiquity suggests a common, topographically based principle of forebrain connectivity.

In the cat auditory cortex, five areas have systematically organized maps of characteristic frequency (CF; tonotopic areas) (Imig and Reale, 1980; Rouiller *et al.*, 1991), i.e. the frequency at the lowest sound pressure level that evokes a response. Eight adjoining areas are non-tonotopic, containing auditory responsive neurons that are not systematically organized according to CF (Schreiner and Cynader, 1984; Clarey and Irvine, 1990; He *et al.*, 1997) and/or receiving thalamic input from auditory thalamic nuclei (Woolsey, 1960; Imig and Reale, 1980; Schreiner and Cynader, 1984; Clarey and Irvine, 1990; Rouiller *et al.*, 1991; He *et al.*, 1997) (Fig. 1A). Topographic projections from the medial geniculate body (MGB) (Morel and Imig, 1987) and tonotopic cortical areas (Imig and Reale, 1980) link frequency-matched loci in other tonotopic nuclei and areas (Lee *et al.*, 2004a). Non-tonotopic regions might be presumed *a priori* to have correspondingly less ordered, or even random, extrinsic projections that reflect this lack of tonotopic organization (Winer *et al.*, 1977). The same is true of limbic and association areas, whose broad responses may derive from the convergence of several modalities and systems that might obscure individual topographies (Bowman and Olson, 1988; Shinonaga *et al.*, 1994; Clascá *et al.*, 1997). Alternatively, the lack of CF topography in non-tonotopic, limbic and association areas could also suggest that a metric besides frequency is mapped, perhaps requiring a topographic connectivity as ordered as that in the tonotopic regions. Distinguishing among these possible architectures has general implications for the physiology of the auditory forebrain and perhaps for its ontogeny.

The wide functional range of auditory cortical areas (tonotopic, non-tonotopic, and limbic related) makes them ideal candidates for testing the generality of neocortical topographic connectivity. We analyzed the extrinsic connections of all auditory cortical and associated thalamic regions, and that of the lateral prefrontal area, to obtain a quantitative profile of the range of connectional topography (Lee, 2004). We used two sensitive retrograde tracers injected either within an area or in different areas (Fig. 1B). The topography of thalamic and cortical connections was quantified by three metrics at different anatomical scales: separation, dispersion, and clustering (Fig. 1C-E). At the largest scale, the separation index assessed the correlation between the injection site intervals and those of the major groups of labeling, and served as a global scaling measure of topographic clusters of labeled neurons across the neocortex. At an intermediate scale, dispersion reflects the local

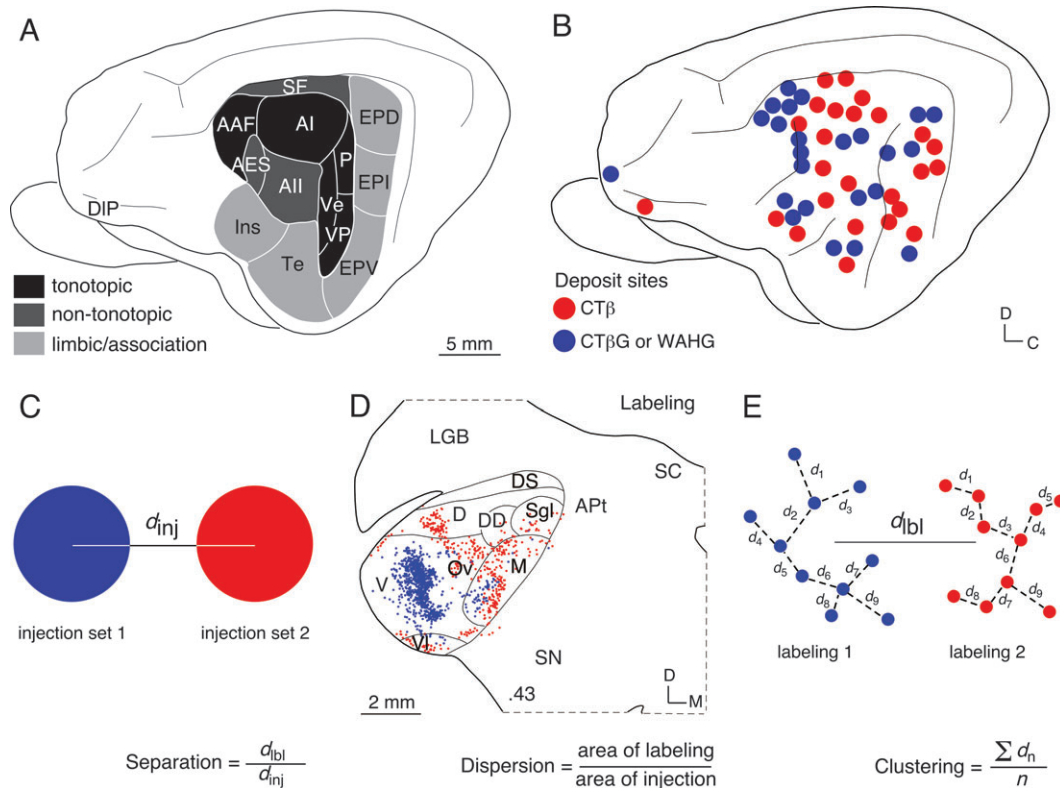


**Figure 1.** Cat auditory cortical areas and experimental design. (A) The cat auditory cortex has at least 13 areas, of which five are tonotopic (black), three are non-tonotopic (dark gray) and five are non-tonotopic, multimodal and limbic-related (gray) (Winer, 1992). (B) To examine projection topography in these areas, two tracers, cholera toxin beta subunit (CT $\beta$ ) (red dots) and wheat-germ agglutinin-*apo*HRP-gold (WAHG) or cholera toxin beta subunit-gold conjugate (CT $\beta$ G) (blue dots), were injected into different cortical loci in each experiment (Table 1, Fig. 2). The standard hemisphere summarizes all injections. Each dot represents the center of a set of injections. (C–E) For topographical analysis, independent measures of convergence, dispersion, and separation were computed. (C) The separation is the distance between the injections sites ( $d_{inj}$ ) relative to the distance between the centers of mass of the labeling ( $d_{bl}$ ). (D) The dispersion index is the ratio of the area of labeling to the area of the injection. (E) The clustering index is the mean distance between a neuron and its closest neighbor. For the experiment in (D): clustering value ( $\mu\text{m}$ ) (CT $\beta$ G/CT $\beta$ ) = 35.4/64.2; dispersion value (CT $\beta$ G/CT $\beta$ ) = 0.36/0.54; separation value = 0.68. Abbreviations used in all figures: AAF, anterior auditory field; AES, anterior ectosylvian area; aes, anterior ectosylvian sulcus; AI, primary auditory cortex; AII, secondary auditory area; APT, anterior pretectum; AS, anterior sylvian area; BIC, brachium of the inferior colliculus; C, caudal; CG, central gray; CL, lateral lateral nucleus; CM, central medial nucleus; CT $\beta$ , cholera toxin beta subunit; CT $\beta$ G, cholera toxin beta subunit gold conjugate; D, dorsal nucleus of the MGB or dorsal; DCa, dorsal caudal nucleus of the MGB; DD, deep dorsal nucleus of the MGB; DIP, dorsolateral prefrontal area; DmP, dorsomedial prefrontal area; DS, dorsal superficial nucleus of the MGB; EN, Edinger-Westphal nucleus; EPD, posterior ectosylvian gyrus, dorsal part; EPI, posterior ectosylvian gyrus, intermediate part; EPV, posterior ectosylvian gyrus, ventral part; Ha, habenula; Illn, oculomotor nerve; Ins, insular cortex; LD, lateral dorsal thalamic nucleus; LGB, lateral geniculate body; LP, lateral posterior nucleus; M, medial division of the MGB or medial; MD, medial dorsal nucleus; mss, middle suprasylvian sulcus; Ov, pars ovoidea of the MGB; P, posterior auditory area; PC, posterior commissure; pes, posterior ectosylvian sulcus; PH, posterior hypothalamus; PL, posterior limitans nucleus; PV, posterior ventral nucleus; R, rostral; Re, reunions nucleus; RN, red nucleus; SC, superior colliculus; SF, suprasylvian fringe (dorsal auditory zone); Sgl, supragenulate nucleus, lateral part; Sgm, supragenulate nucleus, medial part; SII, second somatic sensory area; SMI-32, Sternberger monoclonal antibody 32; SN, substantia nigra; Spf, subparafascicular nucleus; Te, temporal cortex; TRN, thalamic reticular nucleus; V, ventral nucleus of the MGB or ventral; Ve, ventral auditory area; VL, ventral lateral thalamic nucleus; VI, ventral lateral nucleus of the MGB; VM, ventral medial nucleus; VP, ventroposterior auditory area or ventral posterior thalamic nucleus; VPF, ventromedial prefrontal area; Vpm, ventral posteromedial thalamic nucleus; WAHG, wheat-germ agglutinin-*apo* HRP-gold conjugate; 3a, area 3a in primary somatic sensory cortex; 6a $\gamma$ , area 6, lateral division.

spread of labeling and the areal convergence of the projection source to the target. At the finest scale, clustering measured the somatic neural packing density of each projection, and provided an index of topographic continuity. The topographic relations revealed by these measures are highly and equally ordered in tonotopic, non-tonotopic, limbic-related and prefrontal areas, and suggest a singular global topographic principle for the auditory forebrain, and perhaps extending to non-auditory cortex and thalamus as well.

## Materials and Methods

### Surgery, Perfusion, and Histology

Operative procedures were conducted using sterile technique under veterinary supervision and adhered to the guidelines of the University of California at Berkeley animal care and use committee and those of the National Institutes of Health ('Principles of Laboratory Animal Care',

publication no. 85-23). We used standard procedures for anesthesia, surgery, physiology, and histology, as described in an earlier study (Lee *et al.*, 2004a). Briefly, anatomical connectivity in 25 adult, female cats, weighing between 2.8 and 3.5 kg and free of middle ear disease, was studied using deposits of two retrograde tracers, much like the strategy employed in the monkey (Hackett *et al.*, 1999). Deposits guided by physiological mapping were made in four animals (Lee *et al.*, 2004a,b), while 21 others were studied only anatomically (Fig. 2, Table 1). A nanoliter pump (World Precision Instruments, Sarasota, FL) was used to deliver a total volume of 55.2 nl (rate = 4.6 nl/30 s) at depths of 1500, 1000 and 500  $\mu\text{m}$  beneath the pia surface of either of two separate tracers, cholera toxin beta subunit (CT $\beta$ ) (Luppi *et al.*, 1990) and cholera toxin beta subunit conjugated with gold (CT $\beta$ G) (Llewellyn-Smith *et al.*, 1990) (List Biological Laboratories, Campbell, CA), into different sites in one or two areas (9 and 16 cases, respectively) (Fig. 1B). Retrogradely labeled cells from either tracer, as well as double-labeled neurons (Fig. 3D), were readily distinguished from one another (Lee *et al.*, 2004a). Multiple injections of each tracer, termed an injection set (2–3 injection penetrations/tracer/case), were often used

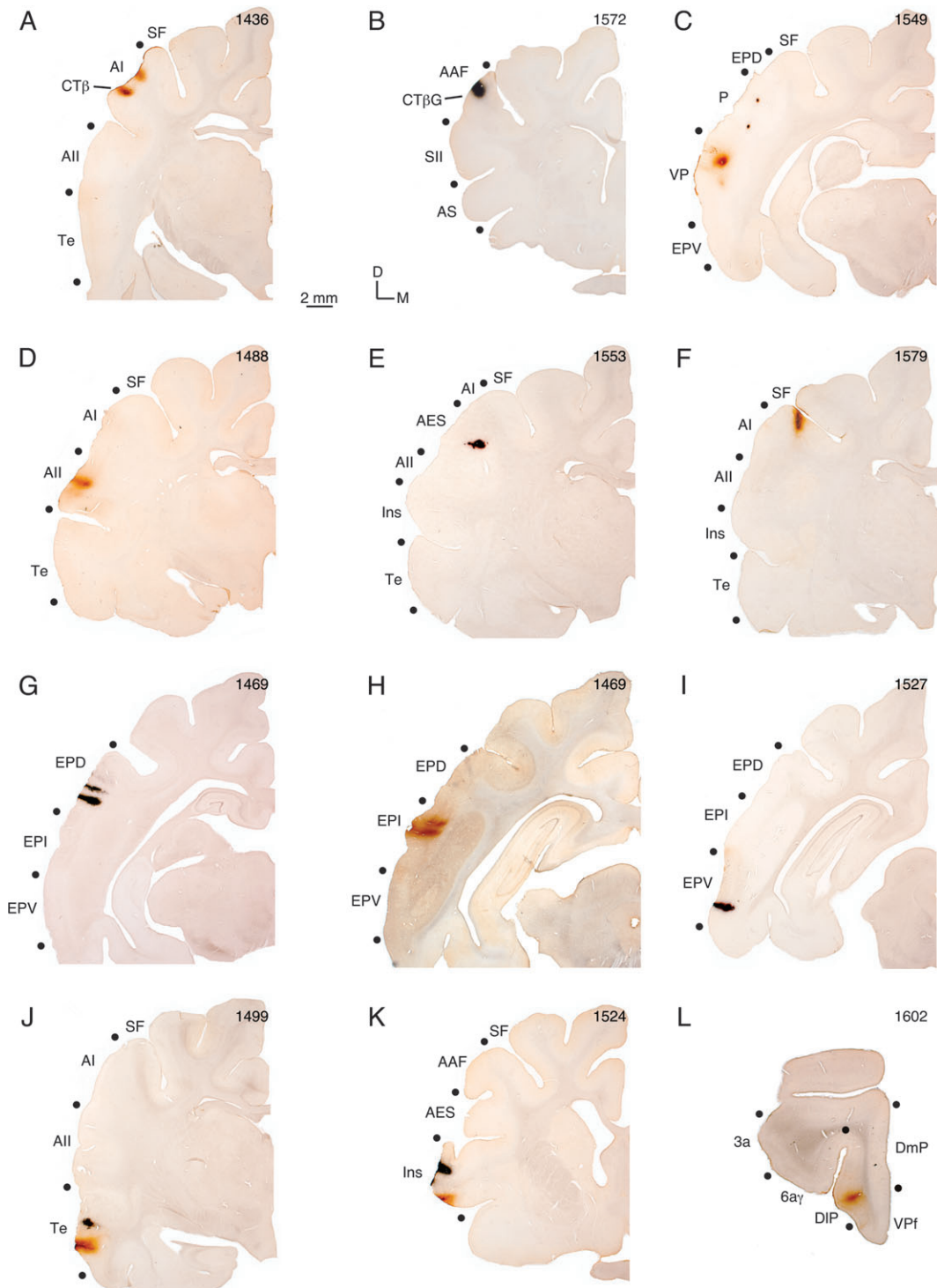


**Figure 2.** Representative injection sites in the auditory areas and prefrontal cortex. Deposits of either cholera toxin beta subunit (CT $\beta$ ) (A, C, D, F, H, J, K, L) and wheat-germ agglutinin-apoHRP-gold (WAHG) or cholera toxin beta subunit-gold conjugate (CT $\beta$ G) (B, C, E, G, I, J, K) were confined to the cortical grey matter and diffused <1 mm. All areas of the cat auditory cortex were investigated. Tonotopic areas: AI (A), AAF (B), P (C), VP (C), Ve (Fig. 3); non-tonotopic areas: All (D), AES (E), SF (F); association regions: EPD (G), EPI (H), EPV (I); limbic regions: Te (J), Ins (K); and the prefrontal cortex (L). See Figure 1 legend for abbreviations. For deposits in sulcal regions, the sulcal banks were gently deflected to allow orthogonal penetrations (C, E, F; Fig. 3B).

due to limited tracer spread (~500–1000  $\mu$ m). In five cases, wheat-germ apo-horseradish peroxidase gold-conjugate (WAHG) (Basbaum and Menetrey, 1987; Winer *et al.*, 1996) was used instead of CT $\beta$ G; the results from the different tracers were indistinguishable.

After 3–5 days (median = 3 days) the animal was perfused with 4% paraformaldehyde/0.01 M phosphate-buffered saline (PBS) and the

brain was blocked stereotaxically, dissected, photographed, and cryoprotected for 3 days in 30% sucrose/4% paraformaldehyde/0.01 M PBS. Frozen sections 60  $\mu$ m thick were cut, and a 1:6 series was processed for each tracer, Nissl preparation and SMI-32 staining, and for plotting and cytoarchitectonic analysis, respectively. To define thalamic nuclear borders and cortical areas, adjacent series were processed with either

**Table 1**

Summary of experiments

Experiment <sup>a</sup>	Case	CTβG/WAHG <sup>b</sup> (no. of injections)	CTβ (no. of injections)	Survival (days)
1	1436	AAF <sup>b</sup> (3)	AI (2)	4
2	1439	AI <sup>b</sup> (3)	AI (2)	3
3	1443	AI <sup>b</sup> (3)	AI (2)	4
4	1444	AI <sup>b</sup> (3)	AI (2)	4
5	1447	EPD <sup>b</sup> (3)	EPI (2)	5
6	1469	EPD (3)	EPI (2)	4
7	1488	EPI (2)	AI (2)	3
8	1499	Te (3)	Te (2)	3
9	1501	AI (3)	Te (2)	3
10	1522	Ins (3)	Ins (2)	3
11	1524	Ins (2)	Ins (2)	4
12	1527	EPV (2)	VP (2)	3
13	1537	AAF (1)	SF (1)	3
14	1549	P (2)	VP (2)	3
15	1553	AES (1)	EPD (2)	2
16	1555	Te (1)	EPV (1)	3
17	1560	Ins (2)	EPD (2)	3
18	1561	AAF <sup>c</sup> (1)	AI <sup>c</sup> (2)	3
19	1568	AAF <sup>c</sup> (1)	AI <sup>c</sup> (3)	3
20	1569	AES (1)	AES (1)	3
21	1572	AAF <sup>c</sup> (1)	AI <sup>c</sup> (3)	3
22	1579	AES (1)	SF (1)	3
23	1599	AAF <sup>c</sup> (1)	AI <sup>c</sup> (3)	3
24	1601	Ve (2)	VP (2)	3
25	1602	PFC (1)	PFC (1)	3

<sup>a</sup>Experiment number.<sup>b</sup>WAHG injections.<sup>c</sup>Physiologically mapped deposit.

the Nissl stain or the SMI-32 antibody (Fig. 3C) (Sternberger Monoclonal Inc., Baltimore, MD). The SMI-32 antibody labels neurofilaments in pyramidal neurons (Sternberger and Sternberger, 1983), and differentially stains each of the 13 auditory cortical areas investigated in this study (Lee and Winer, 2002; Lee, 2004; Mellot *et al.*, 2005), as well as the dorsolateral prefrontal cortex (Cavada and Reinoso-Suárez, 1985).

### Data Analysis

Thalamic boundaries were drawn without knowledge of the labeling. Cytoarchitectonic subdivisions were established by reference to prior work (Winer, 1984b, 1985a). For cortical areas, the SMI-32 immunostaining and the results from prior architectonic studies were available (Rose, 1949; Winer, 1984a,b,c, 1985b; Winer and Prieto, 2001). Deposit sites were reconstructed from adjacent sections. Each injection set (1–3 injections/tracer) was analyzed as a group by constructing a single polygon encircling all injections at their diffusion boundary, which was continuous between injections within the set. The area and centroid of the polygon enclosing the injection set was computed with the Neuroexplorer analysis software (MicroBrightField, Colchester, VT). Labeled neurons were charted using 10–25× objectives on a microscope equipped with the computerized NeuroLucida image-analysis system (MicroBrightField). Cortical labeling was reconstructed using the 3-D solids module in Neuroexplorer (MicroBrightField). Thalamic and cortical plot files were adjusted for shrinkage by 28% and imported to Canvas (Deneba Software Inc., Miami, FL), then aligned with surface and vascular landmarks to superimpose thalamic and cortical boundaries from cytoarchitectonic material. The number of neurons contributing to every projection was quantified, and the major projection in the thalamus and cortex was defined as the projection contributing maximally to the total extrinsic projection in each system, which constituted a unique cluster of neurons comprising >30% of thalamic input, >50% of commissural input, or >20% of corticocortical input.

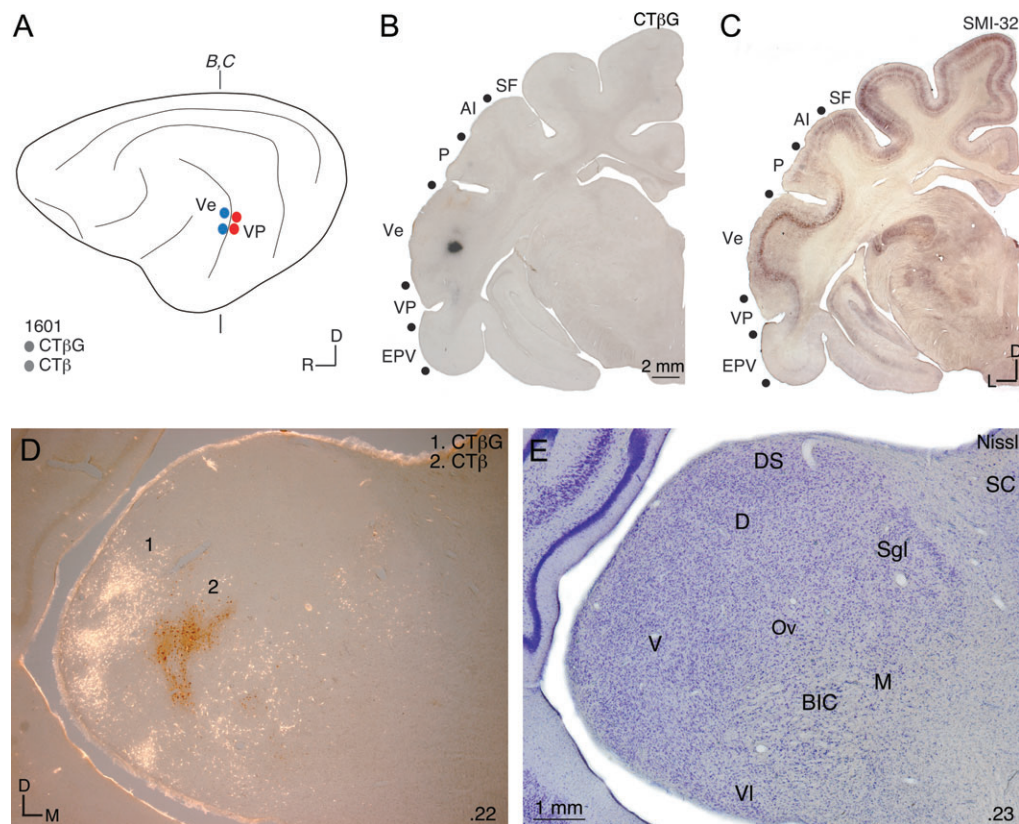


**Figure 3.** Alignment with cytoarchitectonic markers. Areal and nuclear borders were determined from adjacent SMI-32 (Lee and Winer, 2002; Lee, 2004; Mellot *et al.*, 2005) and Nissl (Winer, 1984b, 1985a) material, respectively. For example, in a case with injections of CTβG in Ve and CTβ in VP (A), the cortical injection sites (B) and labeling were closely aligned with adjacent SMI-32 sections (C) to identify areal borders. The resulting thalamic retrograde labeling was highly clustered and topographically segregated (D), and was aligned with the adjacent Nissl material (E) with respect to nuclear borders. See Figure 1 legend for abbreviations.

Measures of the topographic distribution of labeling used the Neuro-explorer analysis software.

The distance between the center of gravity of the major projections and that of the injection sites provided the scaling measure:

$$\text{separation} = d_{\text{bl}}/d_{\text{inj}}$$

where  $d_{\text{bl}}$  represents the distance between the labeling centers and  $d_{\text{inj}}$  represents the distance between injection centers. This relation is graphed such that  $d_{\text{bl}}$  is a function of  $d_{\text{inj}}$  and the slope of the regression line gives an estimate of the overall separation index. The correlation between the injection site intervals and those of the major groups of labeling served as a global scaling measure of topographic clusters across the neocortex.

Dispersion provided a measure of the spread of labeling, and was computed from a ratio of the area of the major projection and the area of the injection:

$$\text{dispersion} = \text{area of labeling}/\text{area of injection}$$

For thalamic labeling, a solid contour of labeling was constructed around the major projection and a cross-sectional area computed along the two longest axes. This index reflected the local spread of labeling and measured the areal convergence of the projection source to the target.

A nearest neighbor algorithm computed clustering, which was defined as:

$$\text{clustering} = \sum d_n/n$$

where  $d_n$  is the distance between a given labeled neuron and the closest neighboring labeled neuron, and  $n$  is the total number of such distances. This measure provided an index of topographic continuity from the somatic neural packing density of each projection.

Graphs of all distributions were produced with Excel (Microsoft Corp., Redmond, WA), and statistical analysis performed using Prism (GraphPad Software, San Diego, CA).

## Results

Injection placement in each of the 14 cortical areas studied was guided by sulcal landmarks and, in four experiments, by physiological maps (Fig. 2). A *post hoc* analysis excluded injections that did not span all cortical layers, that entered the white matter, or were not confined to areal borders whose limits were assessed by SMI-32 antibody and Nissl stains (Fig. 3).

### All Extrinsic Projections are Topographic

In every experiment, the pattern of thalamic and cortical retrograde labeling was clustered and topographic. This was apparent in thalamic sections following injections in both tonotopic (Fig. 4A) and non-tonotopic (Fig. 4B-E) regions. Segregated clusters of thalamic (Fig. 4) and cortical (Fig. 5) cells project separately to each injection site, and a few neurons (<3%) were double labeled (Lee *et al.*, 2004a). Input to the primary auditory cortex (AI) from the ventral division (V, Ov) of the medial geniculate body (MGB) was consistent with the characteristic frequency (CF) gradient in the MGB (Morel and Imig, 1987) (Fig. 4A). The lateral-to-medial dispersion of MGB labeling after AI deposits was consistent with known projection patterns in both the thalamus and cortex (Morel and Imig, 1987; Rouiller *et al.*, 1991; Lee *et al.*, 2004a). By comparison, after deposits in auditory regions devoid of CF maps, such as AII, Te, Ins, and AES, equally clustered and topographic projections arose from the MGB for each (Fig. 4B-E). For instance, dorsal nucleus (D) projections to different domains in AII (Fig. 4B) had a range of clustering, convergence, and separation topographies (Fig. 1C-E) indistinguishable from the values in tonotopic fields (Fig. 7). Minor labeling was found in V, which may result from encroachment of the injections into Ve (Fig. 4B). Dorsal caudal

nucleus projections (DCa) followed similar metrics after injections in Te (Fig. 4C), as did labeling in the suprageniculate (Sgl, Sgm) and other dorsal division nuclei (deep dorsal nucleus: DD) after deposits in the insular (Ins) and anterior ectosylvian (AES) areas, respectively (Fig. 4D,E). Each of these areas is thought to be devoid of connective topography (Clarey and Irvine, 1990; Shinonaga *et al.*, 1994; Clascá *et al.*, 1997). Finally, deposits in the dorsolateral prefrontal cortex (DIP), a region involved in cognitive tasks and the evaluation of internal modes of action and unrelated to audition (Nauta, 1972), labeled loci topographically in the ventral medial and midline thalamic nuclei (Fig. 4F: Vm, CM), suggesting that the projection patterns seen in auditory cortex may occur in non-sensory neocortex.

A similar pattern of topographic connectivity was also present in cortical projections, as shown in representative tonotopic (AI) and non-tonotopic (Te) experiments (Fig. 5). In both cases, topographic cortical projections arose in several ipsilateral (Fig. 5A,B) and contralateral (Fig. 5C,D) areas. Ipsilateral input to AI came mainly (~90%) from other tonotopic regions (AAF, P, VP and Ve). Input to different AI domains was consistent with the physiologic tonotopic gradients of low-to-high frequency in each, e.g. dorsoventral in P, and rostrocaudal in AAF (Imig and Reale, 1980). Unexpectedly, projections to subregions of Te were equally clustered (Fig. 7B) and topographic (Fig. 7E), and originated principally (~80%) from other non-tonotopic regions (AII, Ins, EPI, EPV) (Fig. 5B). In all experiments, the predominant commissural input (>70%) arose from a restricted, homotopic region corresponding closely, but not completely (Fig. 5C: P; Fig. 5D: EPI), to the ipsilateral injection site (Fig. 5A,B).

### Topographic Projections across Multiple Areas

Projections to different areas also were topographic and segregated. The major inputs from the thalamic or cortical sources arose in largely separate nuclei or areas. Interestingly, even two projections from the same nucleus or area were topographically segregated. For example, when frequency-matched (3 kHz) loci in two tonotopic regions are injected (Fig. 6A, circles), largely segregated thalamic (Fig. 6A) and cortical sources (Lee *et al.*, 2004a) were labeled, even though such projections might be expected to commingle. This is consistent with the few (<3%) double-labeled neurons (Lee *et al.*, 2004a). Overlap regions, as in Ov (Fig. 6A), were highly clustered, but differed in the degree of this nuclear micro-segregation. A further and comparable example of such nuclear segregation is seen after injections in two non-tonotopic regions, Ins and EPD (Fig. 6B). While the areas are unrelated physiologically and have independent functional affiliations (Bowman and Olson, 1988; Clascá *et al.*, 1997), the labeling is still topographic and segregated in the thalamus (Fig. 6B) and cortex (Lee, 2004).

### Metrics of Connectional Topography

Three metrics were used to quantify topography. Clustering, dispersion, and separation indices were computed for all (thalamic, ipsilateral, and contralateral cortical) projections (see Methods) (Figs. 1C-E and 7). For tonotopic, non-tonotopic, and limbic/association areas, the range of the descriptive measures of topography was statistically indistinguishable ( $P > 0.05$ ,  $z$ -test) (Fig. 7A-F), indicating that these different functional areas are ordered by the same metric. Comparison of injections within the same area that use either different

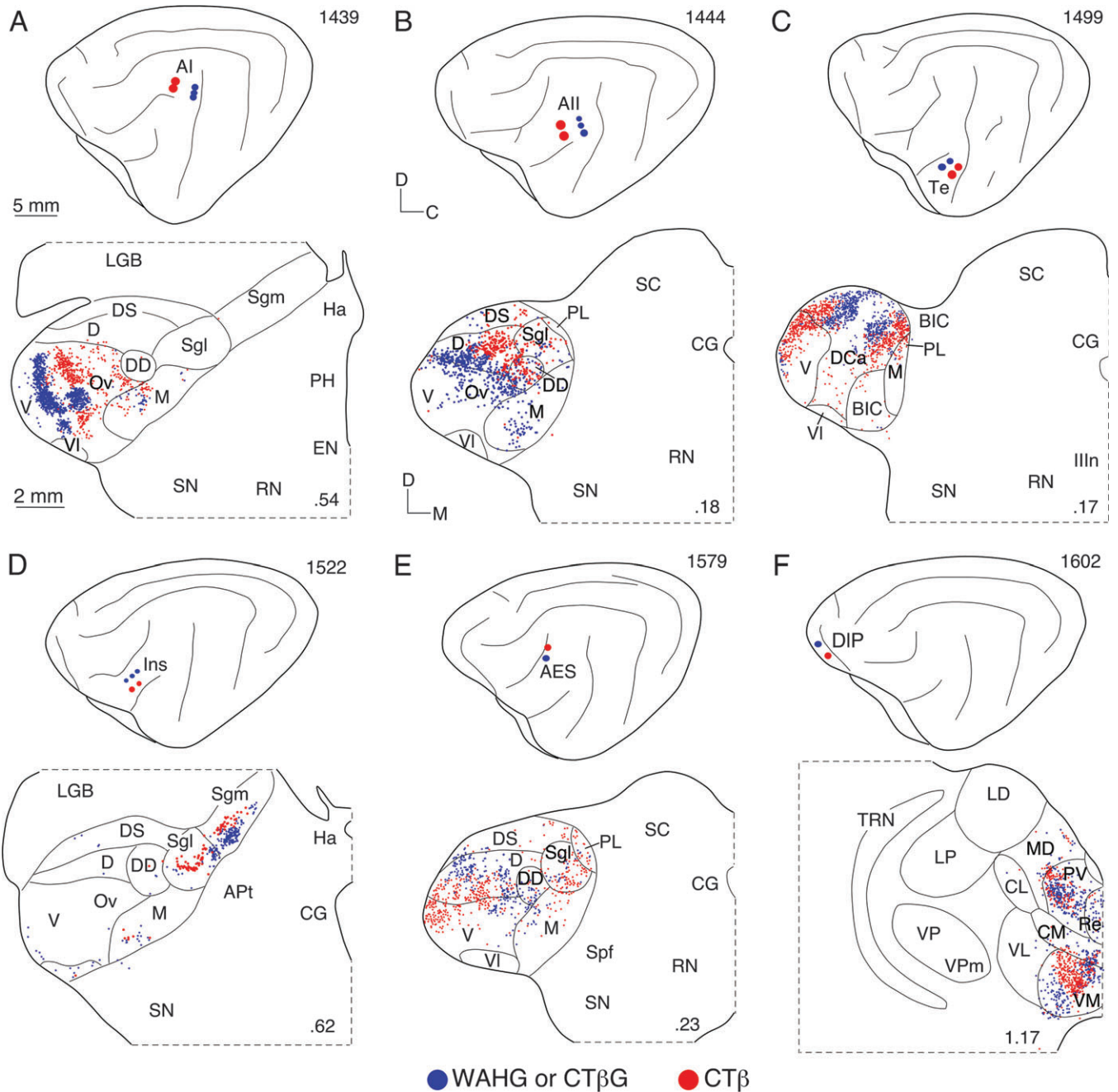


**Figure 4.** All cortical areas receive topographic thalamic input as shown in six representative experiments. (A) Tonotopic areas (AI) have projections whose order is statistically indistinguishable from that of non-tonotopic areas (B: All; C: Te; D: Ins; and E: AES). (F) The topography of thalamic input in the DIP approximates that in auditory cortex. Clustering values (in  $\mu\text{m}$ ) for CT $\beta$ G/CT $\beta$ : A, 30.0/54.4; B, 61.1/57.5; C, 52.3/73.1; D, 53.2/69.1; E, 72.6/79.0; F, 57.3/51.5. Dispersion values (CT $\beta$ G/CT $\beta$ ): A, 1.09/1.23; B, 0.52/0.48; C, 0.72/1.25; D, 1.44/1.23; E, 0.64/0.47; F, 0.89/1.00. Separation values: A, 0.36; B, 0.28; C, 0.47; D, 0.30; E, 0.34; F, 0.27. Decimals in lower right corner indicate the percent distance from the caudal tip of the MGB. See Figure 1 legend for abbreviations.

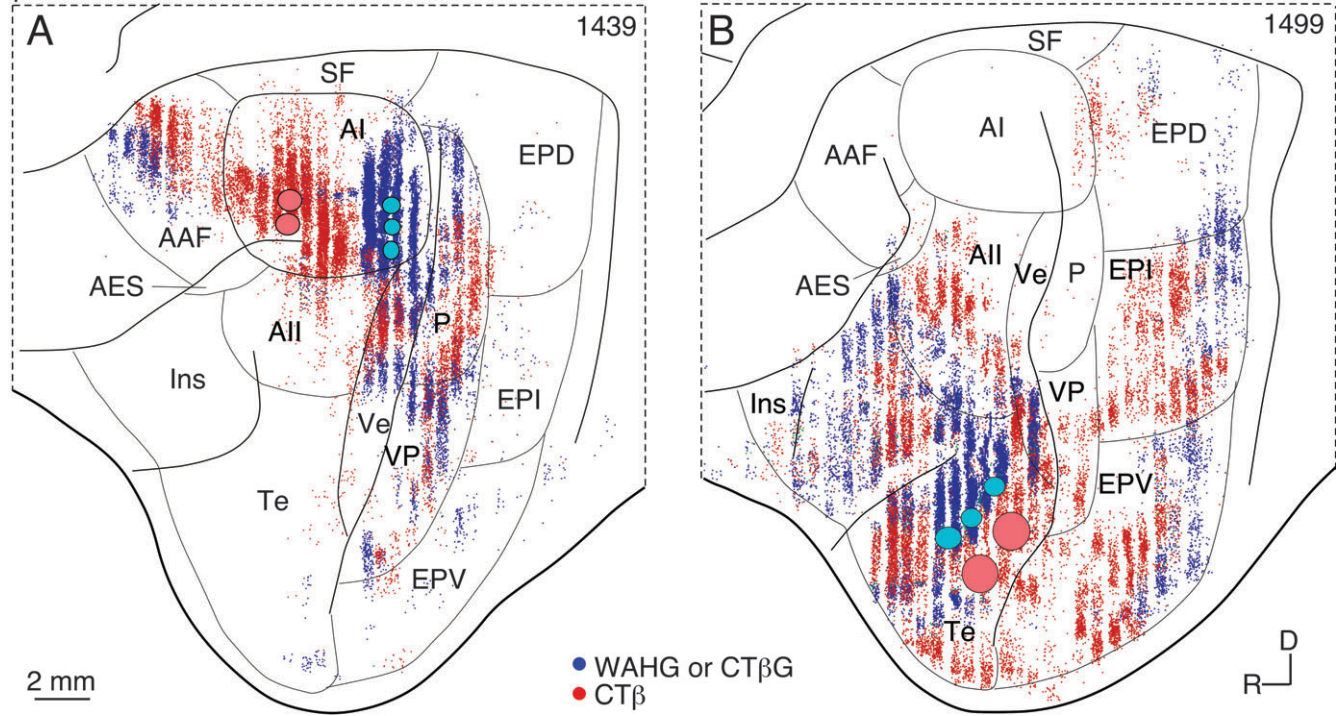
tracers or number of deposits yields results that do not differ significantly from each other ( $P > 0.05$ ,  $z$ -test), and illustrates the robustness of the results despite methodological variance of deposit size and placement.

Clustering is a measure of projection packing (Fig. 1E), and provides an index of the topographic continuity of the projection. This value was significantly lower ( $P < 0.05$ ,  $z$ -test) in the thalamic projections (61  $\mu\text{m}$ ) compared with the cortical projections (96  $\mu\text{m}$ ) (Fig. 7A-C), likely as a result of the larger cortical volume and different magnification factors, and it is

reflected also by the lower variance of the cortical values (Fig. 7B,C).

The dispersion index is the ratio of the area of the projection zone to the area of the target (Fig. 1D), and it was also significantly lower ( $P < 0.05$ ,  $z$ -test) in the thalamus (0.71) compared with the cortex (1.02) (Fig. 7A-C). The thalamic value is slightly higher than expected considering its smaller size; however, the cortical value supports the notion that the ipsilateral and contralateral cortex projections originate from equivalent extrinsic areal domains.

Ipsilateral



Commissural

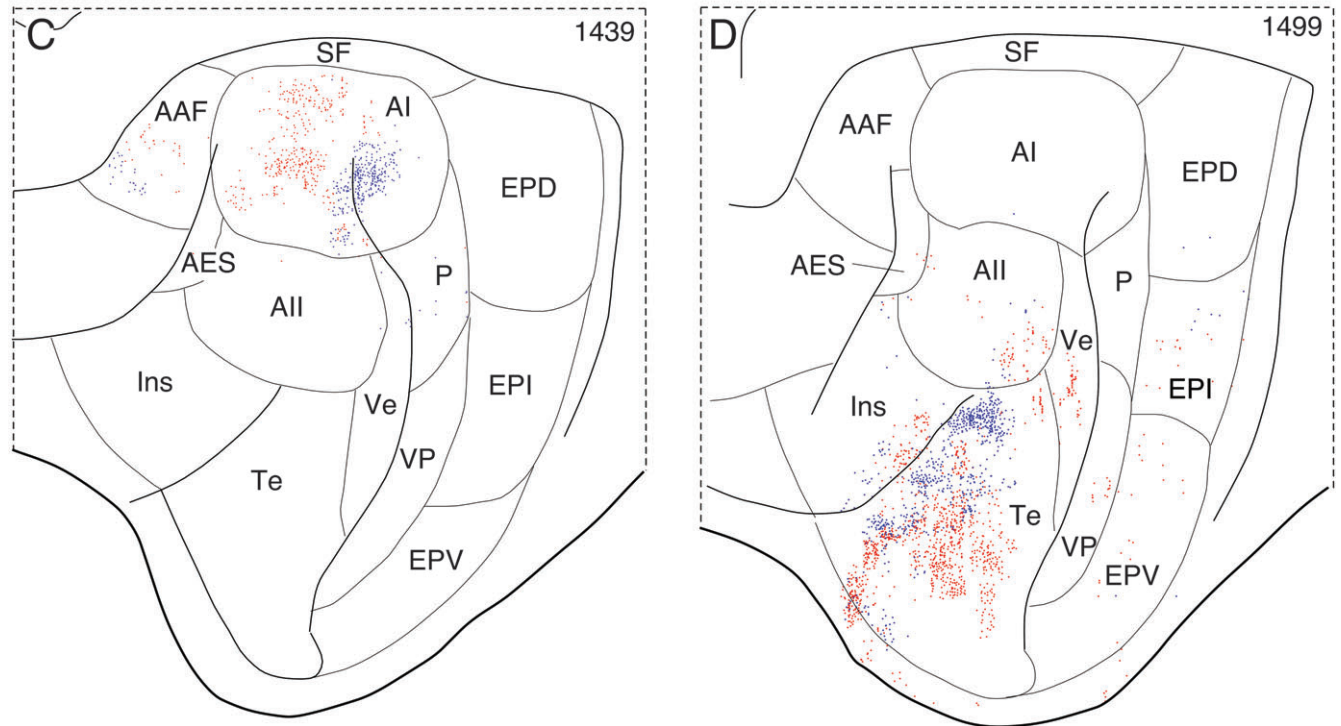


**Figure 5.** (A, B) Ipsilateral and (C, D) commissural projections in the same experiments (cf. Fig. 4) are also topographic. Vertical banding of labeling is an artifact of the reconstruction and the placement of the labeled neurons onto the cortical convexity. Comparing tonotopic (A, C: AI) and non-tonotopic (B, D: Te) projections demonstrates that they are equally topographic in each major forebrain system. In AI (A), ipsilateral cortical projections arise mainly from other tonotopic regions (AAF, P, VP, Ve), whereas those to Te (B) originate from other non-tonotopic areas (All, Ins, EPI, EPV). The commissural projections arise from homotopic loci in the contralateral hemisphere (C, D). Clustering values (in  $\mu\text{m}$ ) (CT $\beta$ G/CT $\beta$ ): A, 83.8/89.5; B, 70.8/84.5; C, 96.5/97.8; D, 128.4/107.7. Dispersion values (CT $\beta$ G/CT $\beta$ ): A, 0.67/0.98; B, 0.88/1.17; C, 1.05/0.98; D, 0.88/1.01. Separation values: A, 0.85; B, 1.01; C, 0.91; D, 1.20. See Figure 1 legend for abbreviations.

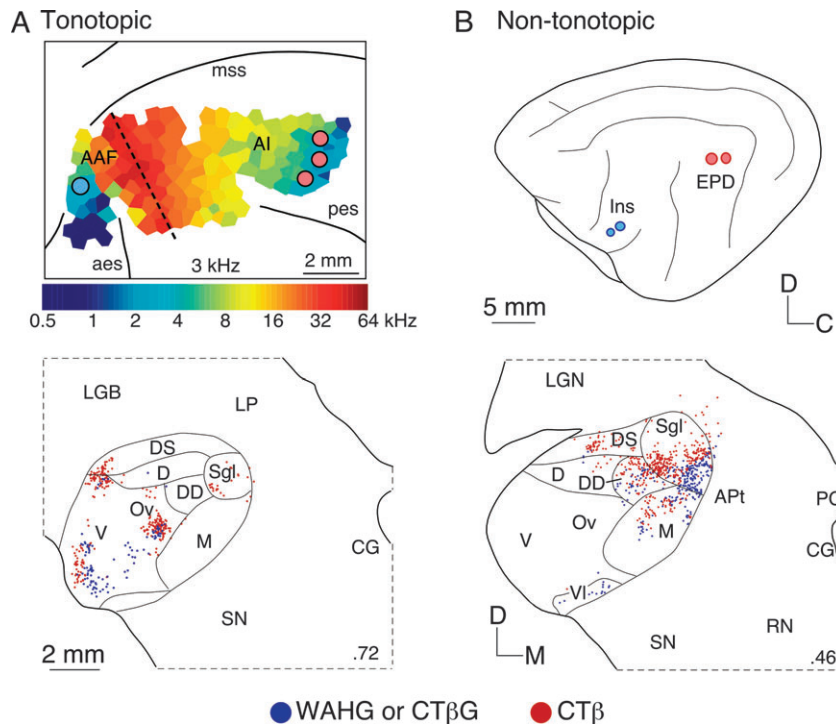


**Figure 6.** Projections compared between physiologically matched and unrelated regions are also topographically segregated. Projections to different areas originate from separate nuclei and areas, but projections from shared nuclei and areas exhibit local segregation of input. (A) Injections placed in tonotopically matched locations in AI (red circles) and AAF (blue circle) label segregated thalamic loci in the ventral division of the MGB. (B) A similar pattern is seen from injections in Ins (red circles) and EPD (blue circles), with segregated projections originating from the supragenulate nuclei (Sgl, Sgm). Clustering values ( $\mu\text{m}$ ) (CT $\beta$ G/CT $\beta$ ): A, 55.1/44.2; B, 51.1/73.0. Dispersion values (CT $\beta$ G/CT $\beta$ ): A, 0.80/0.98; B, 1.32/0.91. Separation values: A, 0.36; B, 0.49. See Figure 1 legend for abbreviations.

Comparison of labeling separation with the deposit separation provides the scaling of projections in each system (Fig. 1C). Compared with cortical projections, thalamic projections were scaled by ~33%, e.g. a 1 mm thalamic separation represents a 3 mm cortical separation (Fig. 7D,E). Commissural projections were the most highly clustered, arising from uniformly scaled, homotopic contralateral domains (Fig. 7F), while the thalamic projections exhibited the greatest topographic variability (Fig. 7D). Thus, all tonotopic and non-tonotopic areas and the dorsolateral prefrontal cortex have statistically indistinguishable topographic projections from extrinsic thalamic, ipsilateral, and contralateral cortical sources.

### Discussion

We found a topographic arrangement of thalamocortical, corticocortical, and commissural connections that is shared in 13 areas of auditory cortex and eight nuclei in the medial geniculate body. These include all cortical subdivisions and thalamic nuclei that are sufficiently large to permit reliable measures of topographic relations. The results suggest a unifying connectional principle that organizes the entire auditory forebrain, and perhaps beyond.

### Constraints on Interpretation

This result may be influenced by methodological factors. We think this unlikely since we used sensitive tracers that reveal many more projection neurons than deposits of comparable size using older methods (Winguth and Winer, 1986; Matsubara and Phillips, 1988). While transected fibers may contribute slightly to this result (Luppi *et al.*, 1990), the small

volume of the deposits (~1 mm<sup>3</sup>) and their confinement to one architectonic area and to the cortical gray matter would limit this. If tracer had spread appreciably, we should expect to see a degradation of the topography, which was not the case. Nor do multiple injections appear to confound the results. If the observed topography does represent such degradation, then the actual precision of these projections would be remarkable.

We recognize, however, that each metric has limited utility, and the robustness of the current results may yield to finer discriminative measures that would be appropriate in the case of smaller deposits or injections confined to a physiological subregion of cortex (Read *et al.*, 2001). The thrust of this study is the question whether any single metric could capture the connectivity of tonotopic and non-tonotopic areas, and to assess this across many areas, nuclei, and deposits on a global basis. The internal organization of subsets of these connections is another matter and beyond the scope of the present study.

The metrics employed in this study were chosen for both their conceptual power and computational simplicity. Each measure can be viewed as sensitive to different anatomical scales of topography. At the finest scale, clustering provides a measure of the topographic continuity of the projection ensemble; while at an intermediate scale, dispersion establishes the convergent relation between projection source and target. At the largest scale, separation measures the organization of the topographic projections in relation to each other across the cortex. Thus, each measure taps independent aspects of the topographic organization, as evinced by the variance among the three metrics (Fig. 7), and each thus provides an orthogonal basis for comparing the topography in each system.



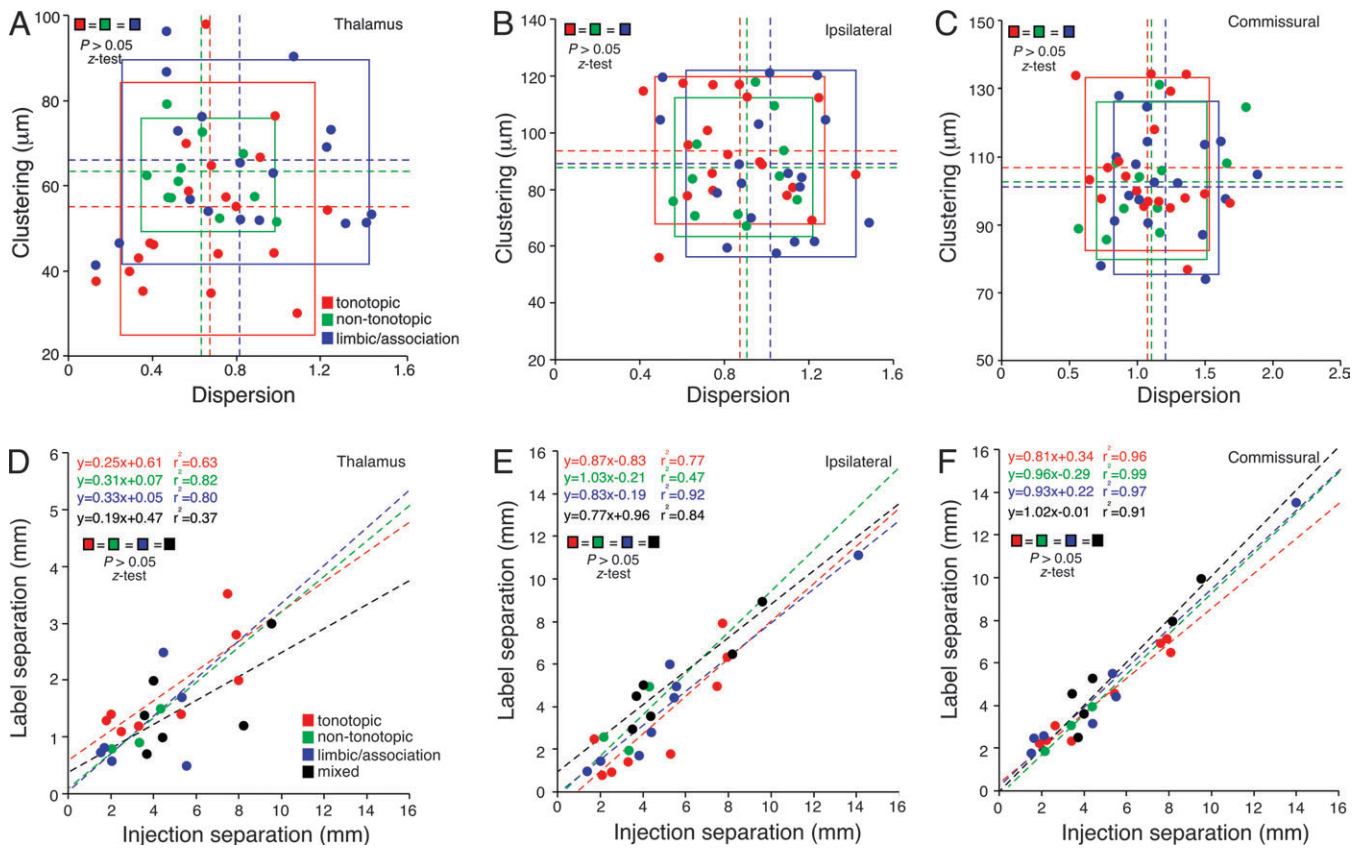


**Figure 7.** Three metrics of topography compared in 25 experiments (50 injection sets). (A–C) The clustering and dispersion indices provide a metric of the specificity of the projection. In each graph, a dot represents the results from one set of injections (see Materials and Methods), dashed lines indicate mean values, and boxes denote 3 SD. In thalamic and cortical projections, clustering and dispersion were the same for tonotopic, non-tonotopic, and limbic/association fields ( $P > 0.05$ , z-test). (D–F) The separation graph shows the scaling of projections in thalamic and cortical pathways. Each dot represents the results of one dual injection experiment. The regression line slopes indicate the average scaling of the main thalamic and cortical projections. In each system, projection scaling is independent of injection locus ( $P > 0.05$ , z-test).

### An Isotropic Connectional Principle

This study reveals an isotropic relation in auditory neocortex and thalamus that includes all areas and nuclear subdivisions investigated, respectively. It thus departs from other forms of local organization, such as ocular dominance, which is limited to certain visual areas (LeVay *et al.*, 1975), or somatic sensory barrels and their representations, which are restricted to specific and singular functional subregions of the trigeminal system (Ma, 1993), ventrobasal complex (Land *et al.*, 1995) and somatic sensory cortex (Woolsey and Van der Loos, 1970). The uniformity and homogeneous distribution of this connectional topography suggests a common principle not limited to specific sensory processing.

Perhaps this topographic principle is a residue of the developmental plan for constructing the forebrain, specifying the sequential and temporal emergence of specific neuronal populations to complete their ontogenetic assignment (Molnár and Blakemore, 1995). The genetic encoding of this topography could ensure that the appropriate thalamic axons are matched with their correct targets, perhaps operating through a general set of chemically specified guidance cues (Grove and Fukuchi-Shimogori, 2003), though such specificity seems absent in some culture regimes (Molnár and Blakemore, 1991).

Such a topographic metric could coordinate the operations of physiologically distinct thalamic nuclei and cortical areas along a common, normalized scale. Interestingly, such scalar relations would supervene across different tonotopic magnification

factors (Schreiner, 1992) as in AI and AAF, which have unique cochleotopic representations (Lee *et al.*, 2004a) and different magnification factors (Imaizumi *et al.*, 2004). Topographic uniformity could thus enable functionally non-equivalent fields to temporally synchronize matched inputs. Such coordinated activation could affect aspects of cortical function ranging from temporal discharge synchrony (Dickson and Gerstein, 1974) to the conditions enabling binding (Treisman, 1999), which presumably require such a topographic connectivity for inter-areal signal propagation.

Multiple physiological representations could be supported by these topographic connections. In AI, the topographic (present results) and tonotopic (Merzenich *et al.*, 1975) frames of reference are aligned, but coexisting representations of binaurality (Middlebrooks *et al.*, 1980) and sharpness of tuning (Read *et al.*, 2001) are interleaved (Ehret, 1997; Read *et al.*, 2001). By comparison, AII contains only a coarse gradient of frequency and binaural segregation appears absent (Schreiner and Cynader, 1984), with similar patterns of limited local segregation prevailing in other cortical subdivisions (Winer, 1992). This suggests that the ontogenetic assembly of AI, where topography is mapped more fully, may be simpler than that in AII and related fields, where less regular physiologic arrangements are superimposed on a topographic scaffold as ordered as that in AI but whose tonotopy is weaker. Alternatively, the physiologic metrics in areas such as AII may be unrelated to the tonotopic framework, and may instead be

derived for computed parameters, as in the midbrain auditory space maps (Masterton, 1992).

Prior connectional studies of auditory cortex have emphasized that thalamic (Winer *et al.*, 1977), commissural (Code and Winer, 1985) and corticocortical (Winguth and Winer, 1986) inputs each have topographic and non-topographic components. Such conclusions were reached without recourse to the simple but robust connectional metrics available in the present study, and are therefore of limited value with regard to topography and precision of projection.

Historically, primary sensory neocortex has been described as having a modular organization (Szentágothai, 1975) and a complementary architectonic homogeneity (Bok, 1959) and isodensity profile, with a few exceptions (Rockel *et al.*, 1980). The topographic arrangement reported here extends this to the scale of global connections and links all extrinsic projection systems to a singular, simple principle. It remains to be seen how far this isotropic principle extends to other sites, systems, and modalities.

## Notes

We thank Drs Christoph Schreiner and Kazuo Imaizumi for the physiological mapping and for their generosity in sharing data from these experiments, David Larue and Tania Bettis for their histological expertise, and Dawn Sung, Richard Lee, Kristen Adams, Haleh Bada-koobehi, and Esther Yoon for assistance with plotting. Drs Christoph Schreiner and Heather Read provided helpful comments on the manuscript. A preliminary report of this work has already been published (Lee and Winer, 2003). This work was supported by USPHS grant R01 DC02319-25.

Address correspondence to Charles C. Lee, Department of Molecular and Cell Biology, Division of Neurobiology, Room 285 LSA, University of California at Berkeley, Berkeley, CA 94720-3200, USA. Email: chazwell@uclink4.berkeley.edu.

## References

- Basbaum AI, Menetrey D (1987) Wheat germ agglutinin-apoHRP gold: a new retrograde tracer for light- and electron-microscopic single- and double-label studies. *J Comp Neurol* 261:306-318.
- Bok ST (1959) *Histonomy of the cerebral cortex*. Amsterdam: Elsevier.
- Bowman EM, Olson CR (1988) Visual and auditory association areas of the cat's posterior ectosylvian gyrus: thalamic afferents. *J Comp Neurol* 272:15-29.
- Cavada C, Reinoso-Suárez F (1985) Topographical organization of the cortical afferent connections of the prefrontal cortex in the cat. *J Comp Neurol* 242:293-324.
- Clarey JC, Irvine DRF (1990) The anterior ectosylvian sulcal auditory field in the cat. I. An electrophysiological study of its relation to surrounding auditory cortical fields. *J Comp Neurol* 301:289-303.
- Clascá F, Llamas A, Reinoso-Suárez F (1997) Insular cortex and neighboring fields in the cat: a redefinition based on cortical microarchitecture and connections with the thalamus. *J Comp Neurol* 384:456-482.
- Code RA, Winer JA (1985) Commissural neurons in layer III of cat primary auditory cortex (AI): pyramidal and non-pyramidal cell input. *J Comp Neurol* 242:485-510.
- Dickson JW, Gerstein GL (1974) Interactions between neurons in auditory cortex of the cat. *J Neurophysiol* 37:1239-1261.
- Ehret G (1997) The auditory cortex. *J Comp Physiol A* 181:547-557.
- Grove EA, Fukuchi-Shimogori T (2003) Generating the cerebral cortical area map. *Annu Rev Neurosci* 26:355-380.
- Hackett TA, Stepniewska I, Kaas JH (1999) Callosal connections of the parabelt auditory cortex in macaque monkeys. *Eur J Neurosci* 11:856-866.
- He J, Hashikawa T, Ojima H, Kinouchi Y (1997) Temporal integration and duration tuning in the dorsal zone of cat auditory cortex. *J Neurosci* 17:2615-2625.
- Hubel DH, Wiesel TN (1962) Receptive fields, binocular interaction and functional architecture in the cat's visual cortex. *J Physiol (Lond)* 160:106-154.
- Imaizumi K, Priebe NJ, Crum PAC, Bedenbaugh PH, Cheung SW, Schreiner CE (2004) Modular functional organization of cat anterior auditory field. *J Neurophysiol* 92:444-457.
- Imig TJ, Reale RA (1980) Patterns of cortico-cortical connections related to tonotopic maps in cat auditory cortex. *J Comp Neurol* 192:293-332.
- Kaas JH (1982) The segregation of function in the nervous system: why do sensory systems have so many subdivisions? In: *Contributions to sensory physiology* (Neff WD, ed.), pp. 201-240. New York: Academic Press.
- Kaas JH (1997) Topographic maps are fundamental to sensory processing. *Brain Res Bull* 44:107-112.
- Kaas JH, Nelson RJ, Sur M, Lin C-S, Merzenich MM (1979) Multiple representations of the body within the primary somatosensory cortex of primates. *Science* 204:521-523.
- Land PW, Buffer SA Jr, Yaskosky JD (1995) Barreloids in adult rat thalamus: three-dimensional architecture and relationship to somatosensory cortical barrels. *J Comp Neurol* 355:573-588.
- Lee CC (2004) Structure of the cat auditory cortex. PhD Dissertation, University of California at Berkeley.
- Lee CC, Winer JA (2002) Commissural connections in cat auditory cortex. *Proc Soc Neurosci* 28:261.
- Lee CC, Winer JA (2003) Topographic projections in cat auditory cortex. *Proc Soc Neurosci* 29:592.
- Lee CC, Imaizumi K, Schreiner CE, Winer JA (2004a) Concurrent tonotopic processing streams in auditory cortex. *Cereb Cortex* 14:441-451.
- Lee CC, Schreiner CE, Imaizumi K, Winer JA (2004b) Tonotopic and heterotopic projection systems in physiologically defined auditory cortex. *Neuroscience* 128:871-887.
- LeVay S, Hubel DH, Wiesel TN (1975) The pattern of ocular dominance columns in macaque visual cortex revealed by a reduced silver stain. *J Comp Neurol* 159:559-576.
- Llewellyn-Smith IJ, Minson JB, Wright AP, Hodgson AJ (1990) Cholera toxin B-gold, a retrograde tracer that can be used in light and electron microscopic immunocytochemical studies. *J Comp Neurol* 294:179-191.
- Luppi P-H, Fort P, Jouviet M (1990) Ionophoretic application of unconjugated cholera toxin B subunit (CTb) combined with immunohistochemistry of neurochemical substances: a method for transmitter identification of retrogradely labeled neurons. *Brain Res* 534:209-224.
- Ma PM (1993) Barrelettes-architectonic vibrissal representations in the brainstem trigeminal complex of the mouse. II. Normal postnatal development. *J Comp Neurol* 327:376-397.
- Malonek D, Tootell RBH, Grinvald A (1994) Optical imaging reveals the functional architecture of neurons processing shape and motion in owl monkey area MT. *Proc R Soc Lond B Biol Sci* 258:109-119.
- Masterton RB (1992) Role of the central auditory system in hearing: the new direction. *Trends Neurosci* 15:280-285.
- Matsubara JA, Phillips DP (1988) Intracortical connections and their physiological correlates in the primary auditory cortex (AI) of the cat. *J Comp Neurol* 268:38-48.
- Mellot JG, van Der Gucht E, Lee CC, Larue DT, Winer JA, Lomber SG (2005) Subdividing cat primary and non-primary auditory areas in the cerebrum with neurofilament proteins expressing SMI-32. *Assn Res Otolaryngol Abstr* 28:994.
- Merzenich MM, Knight PL, Roth GL (1975) Representation of cochlea within primary auditory cortex in the cat. *J Neurophysiol* 38:231-249.
- Middlebrooks JC, Dykes RW, Merzenich MM (1980) Binaural response-specific bands in primary auditory cortex (AI) of the cat: topographic organization orthogonal to isofrequency contours. *Brain Res* 181:31-48.
- Molnár Z, Blakemore C (1991) Lack of regional specificity for connections formed between thalamus and cortex in coculture. *Nature* 351:475-477.
- Molnár Z, Blakemore C (1995) How do thalamic axons find their way to the cortex? *Cereb Cortex* 18:389-397.

- Morel A, Imig TJ (1987) Thalamic projections to fields A, AI, P, and VP in the cat auditory cortex. *J Comp Neurol* 265:119-144.
- Nauta WJH (1972) Neural associations of the frontal cortex. *Acta Neurobiol Exp (Warsz)* 32:125-140.
- Obermeyer K, Sejnowski TJ (2001) Self-organizing map formation: foundations of neural computation. London: MIT Press.
- Peters A, Jones EG (eds) (1985) Cerebral cortex. Vol. 4. Association and auditory cortices. New York: Plenum Press.
- Read HL, Winer JA, Schreiner CE (2001) Modular organization of intrinsic connections associated with spectral tuning in cat auditory cortex. *Proc Natl Acad Sci USA* 98:8042-8047.
- Rockel AJ, Hiorns RW, Powell TPS (1980) The basic uniformity in structure of the neocortex. *Brain* 103:221-244.
- Rose JE (1949) The cellular structure of the auditory region of the cat. *J Comp Neurol* 91:409-440.
- Rouiller EM, Simm GM, Villa AEP, de Ribaupierre Y, de Ribaupierre F (1991) Auditory corticocortical interconnections in the cat: evidence for parallel and hierarchical arrangement of the auditory cortical areas. *Exp Brain Res* 86:483-505.
- Schreiner CE (1992) Functional organization of the auditory cortex: maps and mechanisms. *Curr Opin Neurobiol* 2:516-521.
- Schreiner CE, Cynader MS (1984) Basic functional organization of second auditory cortical field (AII) of the cat. *J Neurophysiol* 51:1284-1305.
- Shinonaga Y, Takada M, Mizuno N (1994) Direct projections from the non-laminated divisions of the medial geniculate nucleus to the temporal polar cortex and amygdala in the cat. *J Comp Neurol* 340:405-426.
- Sternberger LA, Sternberger NH (1983) Monoclonal antibodies that distinguish phosphorylated and nonphosphorylated forms of filament in situ. *Proc Natl Acad Sci USA* 80:6126-6130.
- Szentágothai J (1975) The 'module-concept' in cerebral cortex architecture. *Brain Res* 95:475-496.
- Treisman A (1999) Solutions to the binding problem: progress through controversy and convergence. *Neuron* 24:105-110.
- Tusa RJ, Palmer LA, Rosenquist AC (1978) The retinotopic organization of area 17 (striate cortex) in the cat. *J Comp Neurol* 177:213-236.
- Tusa RJ, Rosenquist AC, Palmer LA (1979) Retinotopic organization of areas 18 and 19 in the cat. *J Comp Neurol* 185:657-678.
- Winer JA (1984a) Anatomy of layer IV in cat primary auditory cortex (AI). *J Comp Neurol* 224:535-567.
- Winer JA (1984b) Identification and structure of neurons in the medial geniculate body projecting to primary auditory cortex (AI) in the cat. *Neuroscience* 13:395-413.
- Winer JA (1984c) The non-pyramidal neurons in layer III of cat primary auditory cortex (AI). *J Comp Neurol* 229:512-530.
- Winer JA (1985a) The medial geniculate body of the cat. *Adv Anat Embryol Cell Biol* 86:1-98.
- Winer JA (1985b) Structure of layer II in cat primary auditory cortex (AI). *J Comp Neurol* 238:10-37.
- Winer JA (1992) The functional architecture of the medial geniculate body and the primary auditory cortex. In: Springer handbook of auditory research. Vol. 1. The mammalian auditory pathway: neuroanatomy (Webster DB, Popper AN, Fay RR, eds), pp. 222-409. New York: Springer-Verlag.
- Winer JA, Prieto JJ (2001) Layer V in cat primary auditory cortex (AI): cellular architecture and identification of projection neurons. *J Comp Neurol* 434:379-412.
- Winer JA, Diamond IT, Raczkowski D (1977) Subdivisions of the auditory cortex of the cat: the retrograde transport of horseradish peroxidase to the medial geniculate body and posterior thalamic nuclei. *J Comp Neurol* 176:387-418.
- Winer JA, Saint Marie RL, Larue DT, Oliver DL (1996) GABAergic feedforward projections from the inferior colliculus to the medial geniculate body. *Proc Natl Acad Sci USA* 93:8005-8010.
- Winguth SD, Winer JA (1986) Corticocortical connections of cat primary auditory cortex (AI): laminar organization and identification of supragranular neurons projecting to area AII. *J Comp Neurol* 248:36-56.
- Woolsey CN (1960) Organization of cortical auditory system: a review and synthesis. In: Neural mechanisms of the auditory and vestibular systems (Rasmussen GL, Windle WF, eds), pp. 165-180. Springfield, IL: Charles C Thomas.
- Woolsey TA, Van der Loos H (1970) The structural organization of layer IV in the somatosensory region (S I) of mouse cerebral cortex. *Brain Res* 17:205-242.